Developmental bias in the evolution of phalanges

Kathryn D. Kavanagh[a], Oren Shoval[b], Benjamin B. Winslow[a], Uri Alon[b], Brian P. Leary[a], Akinori Kan[c,1], and Clifford J. Tabin[c,2]

[a]Department of Biology, University of Massachusetts Dartmouth, North Dartmouth, MA 02747; [b]Department of Molecular Cell Biology, Weizmann Institute, Rehovat 76100, Israel; and [c]Department of Genetics, Harvard Medical School, Boston, MA 02115

Contributed by Clifford J. Tabin, October 3, 2013 (sent for review April 2, 2013)

Evolutionary theory has long argued that the entrenched rules of development constrain the range of variations in a given form, but few empirical examples are known. Here we provide evidence for a very deeply conserved skeletal module constraining the morphology of the phalanges within a digit. We measured the sizes of phalanges within populations of two bird species and found that successive phalanges within a digit exhibit predictable relative proportions, whether those phalanges are nearly equal in size or exhibit a more striking gradient in size from large to small. Experimental perturbations during early stages of digit formation demonstrate that the sizes of the phalanges within a digit are regulated as a system rather than individually. However, the sizes of the phalanges are independent of the metatarsals. Temporal studies indicate that the relative sizes of the phalanges are established at the time of initial cell condensation. Measurements of phalanges across species from six major taxonomic lineages showed that the same predictable range of variants is conserved across vast taxonomic diversity and evolutionary time, starting with the very origins of tetrapods. Although in general phalangeal variations fall within a range of nearly equal-sized phalanges to those following a steep large-to-small gradient, a novel derived condition of excessive elongation of the distal-most phalanges has evolved convergently in multiple lineages, for example under selection for grasping rather than walking or swimming. Even in the context of this exception, phalangeal variations observed in nature are a small subset of potential morphospace.

developmental module | developmental constraint | phalanx

The impacts of modularity and developmental constraint on trait evolvability are enduring themes in evolutionary developmental biology (1–6). Morphological modules are identified as strongly covarying structures; if the source of this covariance is developmental integration, we expect that development will produce a particular subset of phenotypic variations within populations rather than varying in all possible directions (4). This biased set of phenotypes then will influence evolutionary patterns by limiting options for natural selection. Theory suggests that evolution of stable integrated developmental units plays a major role in why we see the set of morphological forms that exist in nature today, in which some integrated developmental units become reinforced over generations and others break apart or reorganize when such innovations are selectively advantageous (4, 5). As a tool to assess modularity and constraint, morphospace, in which measurements are plotted and compared to analyze factors that affect size and shape, is commonly used as a means to compare differences in morphological form, (7).

Modularity in the limb has been widely cited as the basis for the conservation of the basic three-part structure of the limb: the stylopod (upper arm or leg), zeugopod (lower arm or leg), and autopod (hand and wrist or foot and ankle). This structural conservation contrasts with the large range of adaptive variations in size and shape of limb segments among species. How this modular structure and variation apply to the most distal limb parts, the fingers and toes, has not been explored. Digits evolved much later than the antecedents of the more proximal limb structure and are thought to be neomorphic, arising with the invasion of land by amphibians in the Devonian era (8, 9). Clearly, fingers and toes are used for different functions in different species, and the number, size, and shape of phalanges varies tremendously across tetrapod taxa. Bird toes, for example, allow species to grasp prey, perch on branches, run, paddle, or dig. These different functions correlate with different skeletal proportions in the series of phalanges bones. Different positions of the toe joints, which determine proportions, thus are likely to be selectively advantageous for particular lifestyles (Fig. 1*A*).

The extent to which the sizes of the skeletal elements of the limb are truly independent of one another has not been fully explored. Here we address this question from a developmental perspective, focusing on the most distal limb elements, the phalanges.

Results and Discussion

Restriction in the Variation of the Relative Proportions of Phalanges. The phalanges form by a process of sequential segmentation. Cells are added continuously to the distal end of each digit ray from the so-called "digit-forming region" (DFR) at the tip (10). When the newly formed cartilage reaches a critical length, a joint is initiated behind the growing tip, establishing a phalanx behind the new joint, and growth of the digit ray continues distal to the new joint. The skeletal elements of the limb generally are considered to have unique individual developmental identities specified within the three major limb segments. However, whether this modularity applies to the phalanges has been controversial. Some have ascribed a uniquely specified identity to each phalanx (11), whereas others have suggested that the digits are specified as a whole with the phalanges being generated through a reiterative segmentation mechanism in the context of

Significance

It has long been proposed that rules stemming from the mechanisms used during development can constrain the range of evolvable variations in a given form, but few empirical examples are known. We have focused on developmental processes determining proportions of phalanx size along individual digits (fingers/toes) of vertebrates. We find that phalangeal variation seen in nature is indeed constrained by an ancestral developmental program, limiting morphologies to a continuum from nearly equal-sized phalanges to a large-to-small gradient of relative sizes. Nonetheless, later innovations in distal regulation expanded variational possibilities for groups that needed greater grasping ability. These data provide a better understanding of how properties of developmental systems work in combination with natural selection to guide evolution of skeletal proportions.

Author contributions: K.D.K., O.S., and C.J.T. designed research; K.D.K., O.S., B.B.W., U.A., and B.P.L. performed research; A.K. contributed new reagents/analytic tools; K.D.K., O.S., U.A., and C.J.T. analyzed data; and K.D.K., O.S., and C.J.T. wrote the paper.

The authors declare no conflict of interest.

[1]Present address: Orthopedic Surgery, Gifu Central Hospital, Gifu, Gifu 501-1198, Japan.

[2]To whom correspondence should be addressed. E-mail: tabin@genetics.med.harvard.edu.

This article contains supporting information online at www.pnas.org/lookup/suppl/doi:10.1073/pnas.1315213110/-/DCSupplemental.

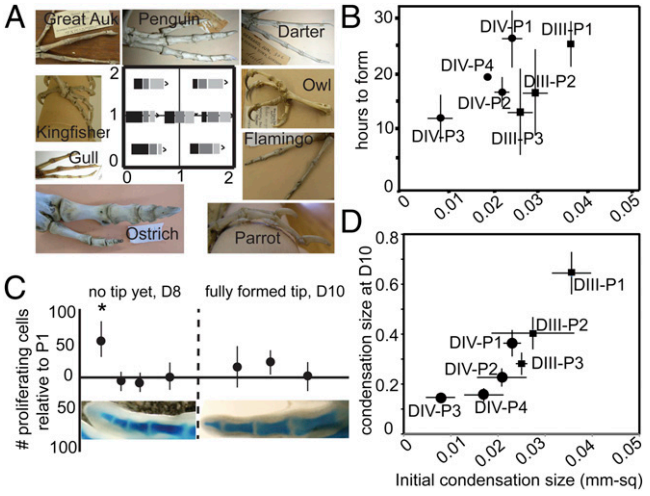

Fig. 1. (*A*) Morphospace potential for bird toe proportions. The *x*-axis shows the ratio of P2/P1; the *y*-axis is the ratio of P3/P1. Black rectangles indicate P1, dark gray rectangles indicate P2, and light gray rectangles indicate P3. The variations in the toe proportions of a variety of skeletal preparations of birds are shown. (*B*) In chick digits the number of hours required for a phalanx to develop from the proximal to the distal joint is related to the size of the initial (distal) condensation. (*C*) Density of proliferating cells (BrdU-incorporated cells) is relatively high in the distal-forming tip of digits, but once the distal joint is formed on a phalanx, proliferation is reduced. No significant differences in proliferation rate are found among formed phalanges within a digit. (*D*) The size of the initial condensation is correlated with size of the condensation when the final pattern is achieved (day 10) in digits III and IV in chicken embryos.

the digit identity (12). To differentiate between these hypotheses, we examined the variation in phalanx size within a single species. We reasoned that if phalanges are specified independently of one another, then the sizes of different homologous phalanges should vary independently among individuals. In contrast, if phalanges are established as part of a developmental module, then their proportions should covary. We measured the 2D area of the first, second, and third phalanges (P1–P3) of the fourth hind limb digit (digit IV) from radiographs of large collections of adult chicken and Zebra Finch skeletons. For each individual we plotted the ratio of P3/P1 versus the ratio of P2/P1, with each individual represented by a single point in morphospace. Strikingly, the plotted ratios for both species fall closely along a single line (Fig. 2*A*). With knowledge of this relationship, one can predict the size of P3 accurately by knowing the sizes of P1 and P2.

To verify that the apparent relationship between phalanges reflects a meaningful developmental integration in the formation of successive digits, we conducted simulations in which phalanx sizes were reassigned in series. The results substantiate that sizes of phalanges are highly unlikely to vary independently ($P < 0.001$) (*SI Appendix*).

Time and Size of Formation of Individual Phalanges. The lack of independence among phalanges suggests that there might be a developmental linkage between the formation of successive phalanges in a growing digit. Previous studies have noted that there is a cyclic oscillation in the expression of the *Hairy2* gene in the developing chick autopod, resembling the activity of the gene segmentation clock during somitogenesis (13). Moreover it was noted that the period of this oscillation, 6 h, is precisely half that of the formation of a phalanx, in particular the second phalanx (P2) of wing digit II, suggesting that phalanges could be generated on a periodic basis every two cycles of a clock (13). If true, this observation might suggest that segments would form at a constant rate and on a constant scale, with differences in phalanx size being attributable to subsequent differential growth. However, this previous study determined the timing of the formation of only a single phalanx.

To address the timing of phalanx formation more generally, we used two approaches. First, we examined specimens from a fine-scale (2-h) time series through phalangeogenesis in chicks. In addition, we removed one foot of a chicken embryo *in ovo*, let the embryo grow a variable (4–48) number of hours, harvested the second foot, and then counted the differences in the number of joints formed in the first and second feet to determine the maximum number of hours between the formation of the proximal and distal joints of a given phalanx (*SI Appendix*). Both sets of observations showed that there is clear variation in the number of hours required to form different phalanges, with the phalanges that ultimately will be the largest having the longest period of formation (~25 h), and the smaller phalanges having significantly shorter periods (8–15 h) (Fig. 1*B*).

The difference in the timing of formation of the different phalanges could, in principle, reflect distinct rates of the condensation process in different elements; alternatively, the difference could be attributable to distinctions in the size of the condensations when they first form. To address these possibilities, we next measured condensation sizes in 161 chicken embryos and 168 Zebra Finch embryos that had been fixed during the period of phalangeogenesis and then stained with Alcian Blue cartilage stain and cleared with KOH. The smallest condensation size was determined by measuring the area of condensation just after the proximal joint of the phalanx was initiated. Down-regulation of cartilage matrix precedes formation of the joint interzone (i.e., the Alcian Blue staining becomes clear), and thus the earliest stages of joint position can be seen easily in Alcian Blue-stained hind limbs. In evaluating whether our sample size was sufficient to detect the initial condensations, we considered that five samples within 5% of the smallest measurement indicated a sampling level at which the smallest initial condensation size was known with confidence (*SI Appendix*). We found that initial condensation sizes differed among phalanges and were significantly correlated with final phalanx size ($P < 0.0001$, ANOVA) (Fig. 1*D*).

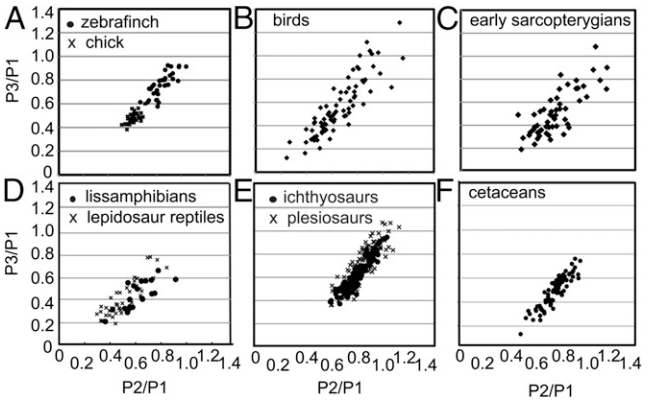

Fig. 2. Variation in proportions of phalanges within and among vertebrate groups. All groups vary along a line from equal-sized to a proximodistal gradient. Ratios are taken from area measurements and are standardized against the size of the first phalanx. *x*-axis: P2/P1; *y*-axis: P3/P1. Plots of the proportions of individual phalanges are for digit IV, P1–3 in (*A*) individual Zebra Finch and chick populations, (*B*) birds, (*D*) lissamphibians, and reptiles. In hyperphalangic (*C*) early sarcopterygians, (*F*) cetaceans, (*E*) ichthyosaurs, and plesiosaurs, the plots are ratios of multiple sets of three sequential phalanges. Equations for the lines are Zebra Finch, $y = 0.7528 + 0.1412$, $r^2 = 0.43$; chick, $y = 0.63 \times 0.03$, $r^2 = 0.49$; $P < 0.0001$; birds, $y = 1.147 \times -0.19$, $r^2 = 0.77$; early sarcopterygians, $y = 0.944 \times -0.17$, $r^2 = 0.62$; lissamphibians, $y = 0.743 \times -0.03$, $r^2 = 0.605$; reptiles, $y = 0.949 \times -0.08$, $r^2 = 0.723$; cetaceans, $y = 1.21 \times -0.39$, $r^2 = 0.825$; ichthyosaurs, $y = 1.23 \times -0.32$; $r^2 = 0.71$; plesiosaurs, $y = 1.327 \times -0.44$; $r^2 = 0.854$.

Although different phalanges form on a scale proportional to their final size, differences in the lengths also could be influenced by differential rates of growth. Therefore, we next used BrdU incorporation to evaluate the proliferation rates of the newly formed phalanges to evaluate the alternative hypothesis, i.e., that differing proliferation rates determine differing phalanx sizes. Although there is a higher rate of proliferation in the distal tip, where the DFR contributes cells to the condensation distal to the most recently formed joint, we saw no significant differences in the percentage of proliferating cells within the different phalanges (i.e., segments that have both proximal and distal joints; Fig. 1*C*). Thus, although proliferation may amplify differences in the relative size of the phalanges (larger phalanges having more total proliferating cells), the essential differences in relative phalanx size appear to be determined by the length of time that has elapsed and hence the number of additional cells added to the growing segment before a new joint forms.

Testing Developmental Modularity Within a Digit. Within a given digit, the high degree of correlation in the variation of phalanx size suggested that phalanges are likely to develop as a modular unit. However, the different phalanges within a module are not all the same size but rather decrease successively in size. A parsimonious explanation would be that each phalanx negatively influences the size of the next, to an extent characteristic of each digit. Because we have found that the proportions of the various phalanges are established at the time of prechondrogenic condensation, such a negative influence, if it exists, must act at the time when the cartilage anlagen is first being set aside (14). To test this notion, we inserted a thin foil barrier into the distal phalanx-forming region, sometimes ending up in the forming joint interzone between the first and second phalanx at day 6.5 in the chick. The hope was that such a barrier would effectively block the influence of the proximal differentiating phalanx on the formation of the next. Indeed, such manipulations consistently resulted in the next forming phalanx (P2) being significantly longer than seen in the unoperated contralateral digit ($n = 28/36$) (Fig. 3). This phenotypic effect was rarely seen in wound controls ($n = 2/27$), indicating that the operation itself was not disruptive of phalanx length. Importantly, the impermeable barriers not only affected the next forming phalanx but also led to subsequent phalanges being of extended length, even though they were formed at a distance from the barrier and well after the digit had healed from the manipulation (Fig. 3). In essence, after insertion of the barrier, the still-to-be-formed phalanges behaved as a modular set, seemingly starting a decreasing sequence anew, distal to the barrier. In most cases the overall length of the digit with the barrier insertion was very close to that seen on the contralateral side, indicating that only the modular segmentation process, and not the overall growth parameters, had been affected. In addition, as expected, the terminal phalanx, which is known to be formed by a process different from that forming the proximal phalanges (15), always was unaffected.

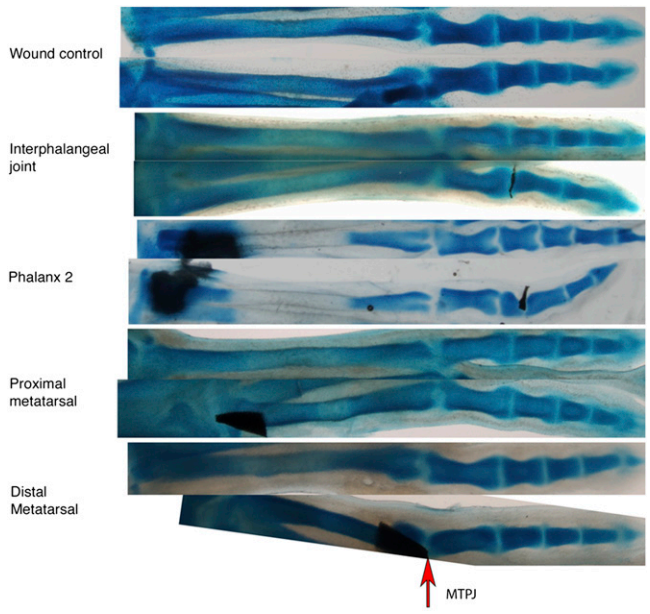

Fig. 3. Barrier experiments. Tantalum foil barriers inserted into developing phalanges affect the size of the distal phalanges. Barriers inserted into developing metatarsals affect metatarsal length but not the patterning of the phalanges. The top digit in each pair is the contralateral control. Proximal is to the left. Images are aligned by metatarsal–phalangeal joint (MTPJ).

Many influential evolutionary studies treat the metapodials as separate from the phalanges, likely because they are observed to vary independently of the loss of the digits (16–18). In contrast to their obvious functional and variational independence from the phalanges within a digit, the morphogenesis of metapodials appears to be exactly the same as that of the phalanges. Thus, the metacarpal and metatarsal bones often are viewed as forming from the same "digital rays" as the phalanges distal to them. No histological or structural differences or differences in gene expression have been reported (19–21). Here, we used an experimental approach to test whether metatarsals are part of the same developmental module as the phalanges. We inserted foil barriers in joint-forming regions between the metatarsal and the presumptive proximal phalanx on day 5.5 of chick development, and embryos were fixed at day 10 when the tip had formed. We found that, although the metatarsals were consistently and variably shortened (25/25 of affected digits were shortened), the phalanges developed normally 100% of the time (Fig. 3). Thus, the metatarsals do not appear to influence the segmentation process forming the phalanges and accordingly appear to be a distinct developmental module.

The Impact of Modular Development on the Evolution of Phalanges. We have found that the phalanges of a given digit are formed as a module. Therefore, although the absolute sizes of homologous phalanges vary within a population, the set of phalanges in any digit maintains predictable size ratios. One consequence of this limit on the range of variation within a population would be a limited range of phenotypes upon which selective forces can act. Thus, in theory, the modular development of the phalanges within a digit would be expected to result in a consequent bias in the evolution of phalangeal patterns. To look at this possibility, we examined the ratios of phalangeal sizes within representative individuals from all available vertebrate taxa that have three or more phalanges in a series (excluding the clawed tip). Area (2D) measurements were taken from digital images of articulated skeletons or fossils or from radiographs of museum specimens. Size proportions were plotted separately for each major group. In some species the sequential phalanges in a given digit are almost the same size, whereas in others there is a dramatic decrease in size from phalanx to phalanx. However, the ratios of the sizes of the phalanges within these digits form a set of proportion variations that is consistent in all taxa (Fig. 2). For example, in birds, when proportions are plotted with P2/P1 vs. P3/P1, the variational distribution of proportions of digit IV, P1–3 in all birds appears to be an extension of the variation found among individuals in chick and Zebra Finch populations (Fig. 2). Statistical analysis shows a high likelihood that both chick and Zebra Finch populations fit the same regression line, which is not detectably different from the regression line for all bird species ($P < 0.0001$) (*SI Appendix*). These results demonstrate that the influence of modular development on variation within bird populations has indeed influenced evolution within class Aves as a whole. The same restriction in phalangeal variation is seen in other taxonomic groups, including land reptiles, plesiosaurs, ichthyosaurs, amphibians, and cetaceans. The variation is limited

so that, by knowing the sizes of two phalanges, one can reliably predict the size of a third.

To see if the developmental integration in the formation of the digital skeleton and the consequent predictability of relative phalanx sizes is a basal feature of tetrapods, we measured the phalanges present in the earliest autopods known from the fossil record, including several extinct amphibian species (22, 23), and from lungfish embryos, because they are a living representative of a basal sarcopterygian, the group from which tetrapod vertebrates evolved (24). The ratios of phalanx sizes in these early autopods are similar to those seen in modern tetrapods, suggesting that the digit skeletal elements have been formed as a developmental module with biased variations since the origination of the autopod, with metapodials later evolving into a separate module. Indeed when each major modern taxon was plotted against basal groups as a whole, no significant differences in slope were observed (Fig. 2 and *SI Appendix*).

Innovation in the Evolution of the Distal Phalanges in Derived Groups. There is one major and very informative exception to this overall pattern. In the hindlimbs of some birds and in the forelimbs of some bipedal dinosaurs and climbing or digging reptiles, the penultimate phalanx (the last phalanx before the tip) is elongated. All these exceptions apparently are coincident with the lack of primary dependence on the limb for propulsion. For example, after examining digital images of a diverse sample of 76 species of birds, P4 of digit IV (and sometimes P3 of digit III) was seen to be significantly longer than anticipated, based on the foregoing analysis, in a number of different species (Fig. 4 and *SI Appendix*). Differences in the relative length of the penultimate phalanx of digits III and IV has been noted previously as a key variable that has been interpreted functionally relative to the lifestyle of birds along a simple spectrum from arboreal to cursorial (25, 26). However, these prior studies did not consider the penultimate phalanges in the context of the overall proportions of the proximal phalanges.

To gain a better understanding of the variation in digit IV, we plotted the data for digit IV in 3D morphospace (plotting the ratios of P2/P1, P3/P1, and P4/P1, along the three Cartesian axes) (Fig. 5 and *SI Appendix*). If digit IV, P4 were regulated independently, all points would be expected to be directly vertical in the z plane above the x–y line. In contrast, we found the observed proportions fell within a roughly triangular plane that was significantly off the vertical. This "tilted" position of the plane results from the observation that, in the species with the most elongated P4s, the P3 is also slightly larger than expected

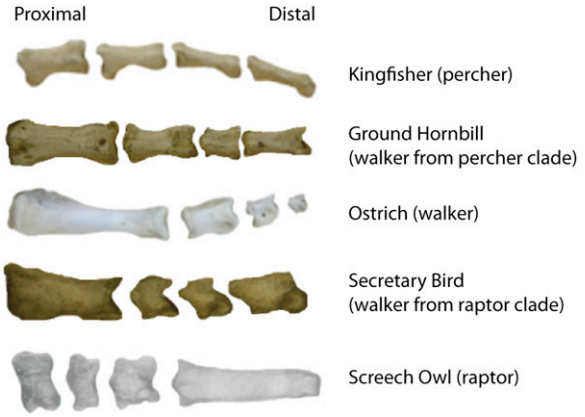

Fig. 4. Examples of convergence in phalanges proportions. From left to right, P1–P4 are aligned; ungual phalanges (tips) have been removed. Phalanges proportions evolve along predicted lines, e.g., the Ground Hornbill, a walking species whose closest taxon is primarily perching, has evolved toward the walking variant by elongating P1 and developing a steeper proximodistal gradient.

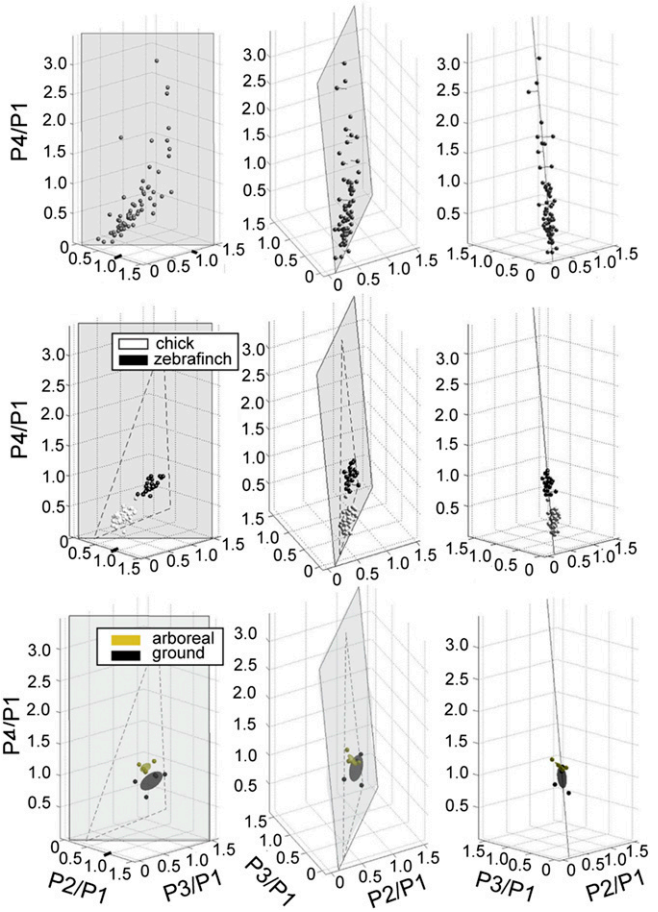

Fig. 5. (*Top*) Phalanges proportions for digit IV in birds fall roughly within a triangular plane in 3D morphospace. (*Middle*) Chick (white dots) and Zebra Finch (black dots) individuals fall within the same morphospace plane as proportion variations among species. (*Bottom*) Galapagos finch species that are more arboreal (yellow) have altered proportions as compared with more ground-dwelling species (black). Ellipses are centroid + 1 SD.

by the basal pattern (see screech owl digit IV in Fig. 4). One plausible developmental model for this pattern of distal elongation would be a response to a distal signal extending growth and delaying segmentation of the distal phalanges superimposed on the general developmental program leading to proportional decrease in sequential phalanx size. As is consistent with this model, the phalangeal elongation we observe is always in the distal-most phalanges. This pattern also is reflected in the triangular shape of the plane, which indicates that some conceivable variations in proportion on the plane are never found in nature (e.g., long-short-long-short). This restricted morphospace is highly improbable unless all phalanges covary as part of the same module (*SI Appendix*) (27). In other words, compared with the majority of vertebrate digits, the distal-most phalanges in birds can become relatively longer than expected from the basal pattern, creating an increased range of variability for these groups. Variation among individuals within populations also falls within this same morphospace (Fig. 5*B*).

We next tested whether particular proportions in birds were correlated with function. Birds were categorized according to known lifestyles or behaviors involving toes of the particular species. The functional categories included raptors, perchers, diggers, walkers, swimmers, and generalists, with species categorized based on published literature. We found that particular proportions in 3D space were associated with particular functional categories

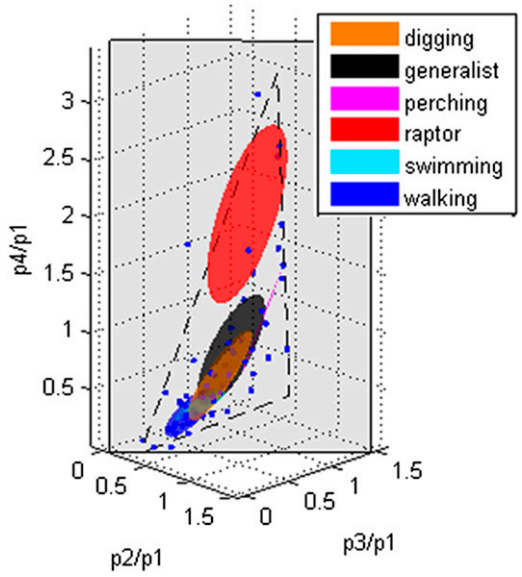

Fig. 6. Ellipses showing the patterns of the phalanges by functional groups established by known lifestyles of the birds. Ellipses are defined by the centroid + 1 SD in all directions for each functional group.

(Fig. 6), with evolution occurring along lines in morphospace that suggest tradeoffs between competing functions (27).

Indeed, by comparing variations found within and between related groups, we found evidence of convergence for function in several groups. For example, the secretary bird (*Sagittarius serpentarius*) is from a raptor clade, but its toes function not only for grasping prey on the ground but also for walking (28, 29). The proportions of the secretary bird's phalanges are intermediate between those of raptors and flightless birds (walkers), with a P1 that is greatly elongated compared with that of any other raptor we measured (Fig. 4). In other words, given sufficient time and selective pressure, the proportions of phalanges in bird digits evolve as a module along predictable lines in morphospace (27), e.g., between optimized walking and grasping functions (Fig. 6).

Thus, despite the highly conserved relationships among phalangeal sizes attained in evolution, when dependence on walking is reduced for a given limb, the distal phalanges appear to be able to elongate dramatically, particularly in association with perching and grasping functions. Moreover, this evolution can occur relatively rapidly. We examined the range of variation in digit IV, P4 in a group of species that have undergone a relatively recent adaptive radiation, the Darwin's finches, which evolved in the Galapagos Islands within the last 3 million years (30). We found that in the more arboreal finches the distal phalanges are more elongated, consistent with the overall correlation between arboreality and P4 length among all birds. The variation in these finches again remains within the predicted plane in 3D morphospace (Fig. 5*C*).

Birds that are diggers, perchers, and raptors have eluded the constrained range of variation in phalangeal proportions through a developmental innovation that apparently has been layered on top of the basal modular phalanx program, allowing greater range of variation in the size of the distal phalanx than otherwise possible. In arboreal and digging mammals, e.g., in Grant's Golden Mole (31) and in certain extinct taxa of sloths (32), this evolutionary challenge has been circumvented differently, by condensing phalangeal elements in normal proportions but then fusing phalanges with one another or with the metapodial to produce a long segment from shorter phalanges. Other arboreal mammals, such as the Two-Toed Sloth (33, 34), have paralleled the digging/perching/predatory birds in extending their distal phalanges to a greater extent than the proximal ones. An insight into at least a potential mechanism by which this extension might have occurred comes from a study (15) in which Fgf signaling was maintained experimentally at the distal tip of a growing digit ray. The result was an elongation of the penultimate phalanx, although the terminal claw was of normal proportions (as is the case in birds with a naturally extended penultimate P4 of digit IV). Thus, one might postulate that, in addition to the modular developmental program influencing the developing phalanges, the length of the phalanges also is positively influenced by signals such as Fgf produced at the tip of the DFR. One also could postulate that maintaining or increasing the level of this distal signal can superimpose an extension of the distal-most phalanges on the normal pattern of regularly decreasing phalanx size.

Conclusions

Although previous studies have reported that proportions of limbs and other skeletal elements are evolvable but are significantly constrained within and between segments (18, 35–37), the

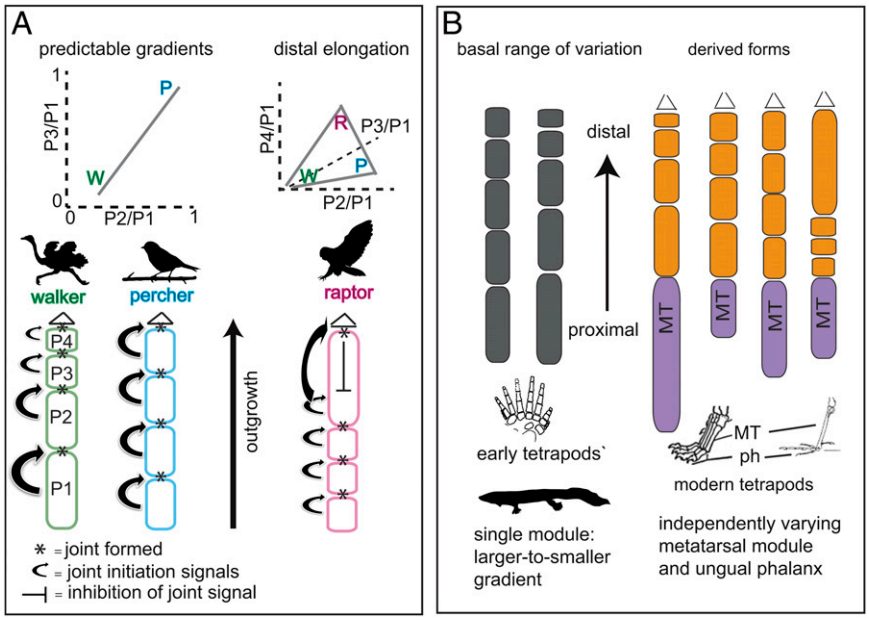

Fig. 7. Summary of results. (*A*) Variants in phalanx proportions remain within a predictable range, from a large-to-small gradient in walkers to equal-sized in perchers to distal elongation of the penultimate phalanx in raptors. Walking and perching specialist phenotypes (W, P) are connected in morphospace by a line, where different phenotypes along the line show a trade off of functions (27). Three functions lead to a full triangle whose vertices are W, P, and the raptor specialist phenotype, R. Joint positions are determined in sequence as the digit grows. Distal elongation may be caused by the inhibition of the joint-initiation signals. (*B*) Hypothesis of origins of modules in the digit. Phalanges in early tetrapods vary as one module, whereas derived tetrapods have two independently varying modules. MT, metatarsal; ph, phalanx.

developmental basis for these observations has been unclear. Focusing on the distal elements of the autopod, we have found that the formation of the phalanges of each digit is specified as a developmental module rather than as a series of independently specified elements. As a consequence, there is a developmental bias, so that in independent vertebrate lineages the proportions of phalanges have evolved repeatedly within a limited subgroup of all possible variations in morphospace (Fig. 7). The variation arises developmentally during a short period of morphogenesis during which joint positioning is established. The scenario we propose involves an ancestral developmental system that allowed variations ranging from equal-sized to a large-to-small gradient, with later innovations in distal regulation that opened up new variational possibilities for groups that needed greater grasping ability. These data thus provide a better understanding of how the properties of developmental systems work in combination with natural selection to guide evolution of skeletal proportions in vertebrates.

Methods

Analysis of Proportions and Morphospace. Adult specimens of birds, reptiles, amphibians, cetaceans, plesiosaurs, ichthyosaurs, and Darwin's finches were obtained from the American Museum of Natural History, the British Museum of Natural History, the Harvard Museum of Comparative Zoology, the Boston Museum of Science, and the Museum of the Rockies (see Dataset S1). Zebra Finch feet were obtained from university research animal colonies. The birds were excess breeders that were part of IACUC approved protocol BU11-026 in an AAALAC approved songbird breeding facility at Boston University; Chicken feet were obtained from Boston Chinese markets. From skeletal preparations and fossils, digital photographs were taken from the dorsal (top) side of the foot; for museum skins, digital X-ray was used to obtain images of phalanges. For some of the early sarcopterygian taxa, which are extremely rare and difficult to access, published photographs or illustrations were used to obtain measurements. Measurements of phalanges areas were made using ImageJ software by tracing around each phalanx. Proportions (P2/P1, P3/P1, and P4/P1) were plotted in 2D or 3D morphospace for visualization of the variation. Using MatLab, principal component analysis data were used to measure variance and to establish the relationships between various sets of proportions. A statistical protocol was used on generated randomized datasets to establish whether the observed relationships between phalanges proportions were statistically significantly different from random (described in detail in *SI Appendix*). Functional data on the use of toes by bird species were obtained from published sources (*SI Appendix*).

Developmental Analyses. We used two methods to calculate the number of hours elapsed between the formation of the proximal joint and the formation of the distal joint in a phalanx. First, several large batches of chick eggs were incubated synchronously, and a 2-h time series was collected and stained with Alcian Blue. Condensation sizes for each phalanx were measured over each time period. The average elapsed time between proximal and distal joint formation was calculated to estimate the time of formation for a given phalanx. A second method involved removing one limb, allowing the embryo to grow for 4–48 h longer, then removing the other limb, performing Alcian staining, and counting the difference in the number of joints. The maximum number of hours before a new joint was observed in a digit was determined by estimating the number of hours required to form a given phalanx. Proliferation rates were calculated by labeling developing embryos with BrdU (Invitrogen EdU kits Alexa Fluor 555) and counting the numbers of labeled cells in 200-μm quadrants. Barrier experiments were conducted using tantalum foil implants into digit IV of chick hindlimbs either on day 5 (metatarsal barriers) or on day 6–7 (phalanges barriers). Embryos were collected at day 10, fixed, and Alcian stained. For wound controls foil barriers were inserted and then were removed about 1 min later. Alcian Blue-stained condensations were measured and compared among treatment groups.

ACKNOWLEDGMENTS. We thank the members of the C.J.T. and K.D.K. laboratories for comments on the research and manuscript, L. Mahler and S. Mallick for assistance with data analysis, C. Koeppl for providing embryos, and the British Museum of Natural History and Museum of Comparative Zoology at Harvard University for access to specimens. This work was supported by National Institutes of Health/National Institute of Diabetes and Digestive and Kidney Diseases Grant P01DK056246 (to C.J.T.) and funds from the University of Massachusetts Dartmouth (to K.D.K.).

1. Atchley WR, Hall BK (1991) A model for development and evolution of complex morphological structures. *Biol Rev Camb Philos Soc* 66(2):101–157.
2. Gould SJ (1977) *Ontogeny and Phylogeny* (Harvard Univ Press, Cambridge, MA).
3. Kirschner M, Gerhart J (1998) Evolvability. *Proc Natl Acad Sci USA* 95(15):8420–8427.
4. Klingenberg CP (2008) Morphological integration and developmental modularity. *Annu Rev Ecol Evol Syst* 39:115–132.
5. Schlosser G, Wagner G (2004) *Modularity in Development and Evolution* (Univ of Chicago Press, Chicago).
6. West Eberhard MJ (2003) *Developmental Plasticity and Evolution* (Oxford Univ Press, New York).
7. Eble GJ (1999) Developmental and non-developmental morphospaces in evolutionary biology. *Morphospace Concepts and Applications*, eds Chapman RE, Rasskin-Gutman D, Wills M (Cambridge Univ Press, Cambridge, UK).
8. Hall BK (2007) *Fins into Limbs: Evolution, Development, Transformation* (Univ of Chicago Press, Chicago).
9. Shubin N, Tabin C, Carroll S (1997) Fossils, genes and the evolution of animal limbs. *Nature* 388(6643):639–648.
10. Suzuki T, Hasso SM, Fallon JF (2008) Unique SMAD1/5/8 activity at the phalanx-forming region determines digit identity. *Proc Natl Acad Sci USA* 105(11):4185–4190.
11. Wolpert L (2002) Limb patterning: Reports of model's death exaggerated. *Current Biology* 12(R):R628–R630.
12. Richardson MK, Jeffery JE, Tabin CJ (2004) Proximodistal patterning of the limb: Insights from evolutionary morphology. *Evol Dev* 6(1):1–5.
13. Pascoal S, et al. (2007) A molecular clock operates during chick autopod proximal-distal outgrowth. *J Mol Biol* 368(2):303–309.
14. Hartmann C, Tabin C (2001) Wnt-14 plays a pivotal role in inducing synovial joint formation in the developing appendicular skeleton. *Cell* 104(3):341–351.
15. Sanz-Ezquerro JJ, Tickle C (2003) Fgf signaling controls the number of phalanges and tip formation in developing digits. *Curr Biol* 13(20):1830–1836.
16. Gatesy SM, Middleton KM (1997) Bipedalism, flight and the evolution of theropod diversity. *J Vertebr Paleontol* 17:308–329.
17. Shapiro M, Hanken J, Rosenthal N (2003) Developmental basis of digit loss in the Australian lizard *Hemiurgis*. *J Exp Zool B Mol Dev Evol* 297:48–56.
18. Young NM, Wagner GP, Hallgrímsson B (2010) Development and the evolvability of human limbs. *Proc Natl Acad Sci USA* 107(8):3400–3405.
19. Guo X, et al. (2004) Wnt/beta-catenin signaling is sufficient and necessary for synovial joint formation. *Genes Dev* 18(19):2404–2417.
20. Settle SH, Jr., et al. (2003) Multiple joint and skeletal patterning defects caused by single and double mutations in the mouse Gdf6 and Gdf5 genes. *Dev Biol* 254(1): 116–130.
21. Storm EE, Kingsley DM (1999) GDF5 coordinates bone and joint formation during digit development. *Dev Biol* 209(1):11–27.
22. Coates MI, Clack JA (1990) Polydactyly in the earliest known tetrapod limbs. *Nature* 347:66–69.
23. Carroll R (2009) *The Rise of Amphibians: 365 Million Years of Evolution* (Johns Hopkins Univ Press, Baltimore).
24. Ahlberg PE 2003. Fossils, developmental patterning, and the origin of tetrapods. *The New Panorama of Animal Evolution*, eds Legakis A, Sfenthourakis S, Polymeni R, Thessalou-Legaki M (Pensoft Publishers, Moscow) pp 44–54.
25. Hopson JA 2001. Ecomorphology of avian and non-avian theropod phalangeal proportions: Implications for the arboreal vs terrestrial origin of birds. *New Perspectives on the Origin and Early Evolution of Birds: Proceedings of the International Symposium in Honor of John H. Ostrom*, eds, Gautheir J, Gall LF (Peabody Museum of Natural History, Yale University, New Haven, CT).
26. Kambic RE 2008. *Multivariate Analysis of Avian and Non-Avian Theropod Pedal Phalanges*. M.S. thesis (Montana State University, Bozeman, MT).
27. Shoval O, et al. (2012) Evolutionary trade-offs, Pareto optimality, and the geometry of phenotype space. *Science* 336(6085):1157–1160.
28. Steyn P (1983) *Birds of Prey of Southern Africa: Their Identification and Life Histories* (Tanager Books, Inc., Dover, NH).
29. Ferguson-Lees J Christie. D. 2001. *Raptors of the World*. (Houghton–Mifflin Company, New York).
30. Grant BR, Grant PR (2002) Lack of premating isolation at the base of a phylogenetic tree. *Am Nat* 160(1):1–19.
31. Kindahl M (1949) The embryonic development of the hand and foot of Eremitalpa (Chrysochloris) grani (broom). *Acta Zool* 30:133–152.
32. Naish D (2005) Fossils explained 51(6): Sloths. *Geology Today* 21:232–238.
33. Mendel FC (1981a) Foot of two-toed sloths: Its anatomy and potential uses relative to size of support. *J Morphol* 170:357–372.
34. Mendel FC (1981b) Use of hands and feet of two-toed sloths (Choloepus hoffmanni) during climbing and terrestrial locomotion. *J Mammal* 62:413–421.
35. Adams DC, Nistri A (2010) Onotogenetic convergence and evolution of foot morphology in European cave salamanders (Family: Plethodontidae). *BMC Evol Biol* Jul 16:10:216.
36. Kavanagh KD, Evans AR, Jernvall J (2007) Predicting evolutionary patterns of mammalian teeth from development. *Nature* 449:427–432.
37. Young NM (2013) Macroevolutionary diversity of amniote limb proportions predicted by developmental interactions. *J Exp Zool B Mol Dev Evol* 320(7):420–427.

Supplementary Appendix

For Kavanagh et al. Developmental Bias in the Evolution of Phalanges

List of Supplementary Material:

SOM 1: Tests of distribution within the morphospace of phalanges proportions.

1A. A test for determining how well the data is distributed on a line.

1B. A test for determining how well the data is distributed on a plane.

1C. Tests for whether a 2-trait dataset stems from the same distribution as another dataset

1D. Results for Bird populations (Chicken and Zebrafinch)

1E. Results for Major vertebrate taxonomic groups

1F. Results for Bird species for Digit IV P1-P4

1G. Statistical significance of digit 4 data being on a plane

1H. Results for Darwin's finches

SOM 2: Developmental methods and analyses

2A. Time for formation of a phalanx from proximal to distal joint interzone.

2B. Proliferation study of developing phalanges

2C. Barrier experiments: Metatarsal vs Phalanges

SOM 1: Tests of distribution within the morphospace of phalanges proportions.

By Oren Shoval

1A. A test for determining how well the data is distributed on a line.

Criterion for linear relationship between traits

Here we present a statistical test of whether a dataset in two dimensions is well described by a line. Principal component analysis (PCA) is used to measure the 'linearity' of the data: PCA returns the variance of the data along the first and second principal components. The ratio between these two variances, $v_r=var(PC_2)/var(PC_1)$, is a measure of the correlation of the data. The lower v_r, the more the data is distributed along a line. As an example, consider the data for the birds dataset Fig. S1. The percent variance of PC1 and PC2 is 94.4% and 5.6%, respectively, yielding $v_r=0.059$.

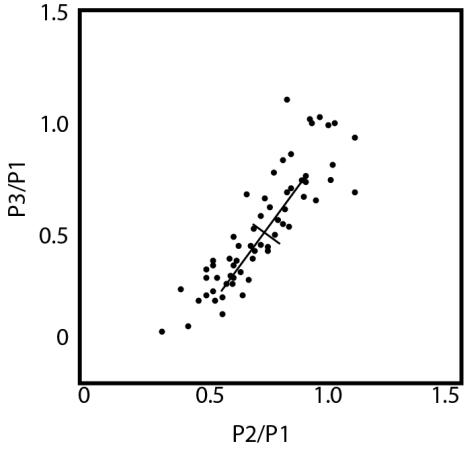

Figure S1. Principal component analysis of the birds dataset. Black lines depict the two principal components. Line length corresponds to the standard deviation (STD) of each component. Crossing point is at average of data in both axes.

Generating a randomized data set

To obtain a statistical significance for the linear-relationship criterion of a dataset, we compare it to a null model - made of an ensemble of suitably randomized datasets. We chose for this purpose a null model that preserves the statistics of each trait, but that reflects a situation where the traits are independent of each other. The null model thus assumes that the two coordinates of the data (x,y) are independent. We generated a large number (10^4) of randomized datasets as follows: each dataset is comprised of the same number of points N as the original dataset. Each point has an x value drawn from the CDF (cumulative distribution function) of the original data's x values, and a y value drawn from the CDF of the original data's y values (Figure S2). We repeat this process until we have the number of points as in the original data set. In this method the null model's x and y CDFs coincide with the CDFs of the x and y of the original data, but we eliminate the relationship between the x and y value (Figure S2). For the randomized dataset 63.8% of the variance is explained by PC_1, 36.2% by PC_2, yielding v_r=0.57, showing that it is significantly less correlated than the original dataset.

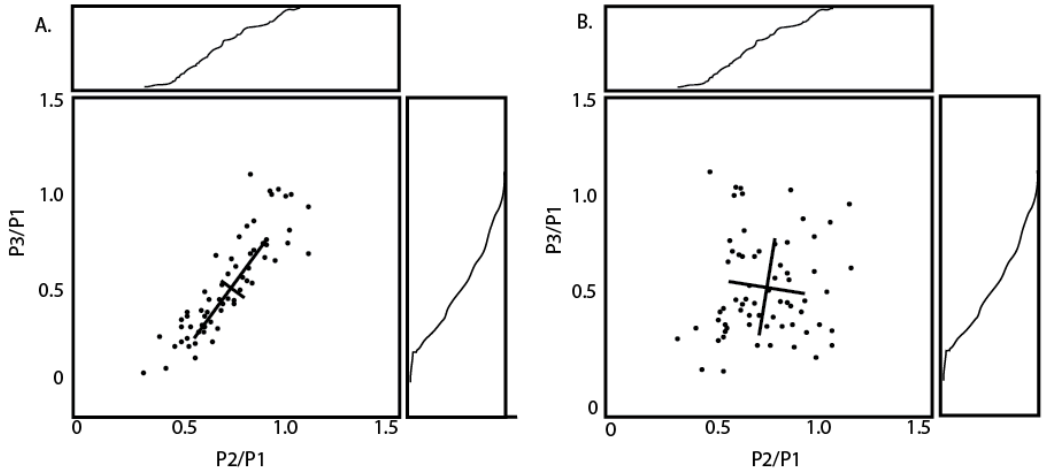

Figure S2. A. Cumulative distribution functions (CDF) of x (P2/P1) and y (P3/P1) values of birds dataset. B. Randomized data set, with CDFs equal to those of the original dataset.

Computing the p-value

To find the p-value for the linearity of a dataset, we first compute v_r - the ratio of variances of the original dataset. We then generate random datasets as described above. For each random dataset we calculate v_r. The resulting p-value is the fraction of randomized datasets for which v_r is lower than the original dataset's v_r. Statistics for 10,000 randomized datasets based on the birds dataset, are shown in Figure S3. Since all 10,000 randomized datasets have a higher v_r, the p-value is smaller than 10^{-4}.

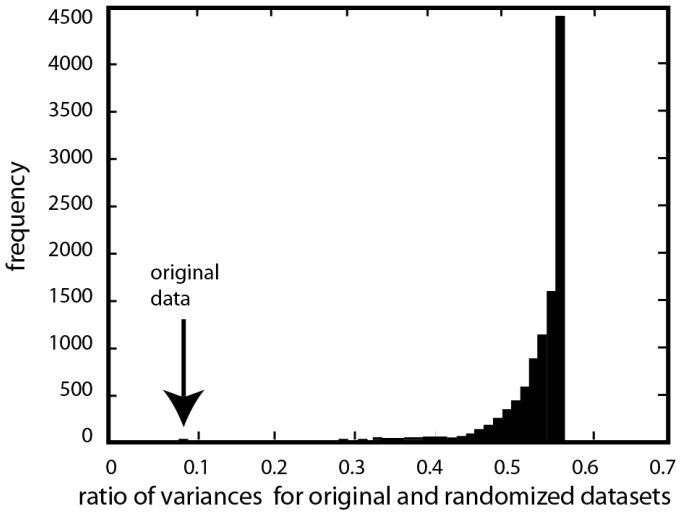

Figure S3. Histogram of v_r – the ratio between variances of the principal components for 10,000 randomized datasets. The original dataset has a v_r value of 0.059, which is lower than the values for all randomized datasets, leading to a p-value < 10^{-4}.

1B. A test for determining how well the data are distributed on a plane.

Criterion for planar relationship between traits

In this case there are three traits – P4/P1, P3/P1, and P2/P1, leading to a three dimensional morphospace. Here, we use a similar method to the one described above in order to analyze how well the data falls on a plane. As a measure, we use the ratio of variances between the 3rd and 2nd PCA components - $v_r=var(PC_3)/var(PC_2)$. As an

example, consider the data for the birds dataset (Figure S4). The percent variance of PC1, PC2, and PC3 is 92.2%, 7%, and 0.8%, respectively, yielding v_r=0.12.

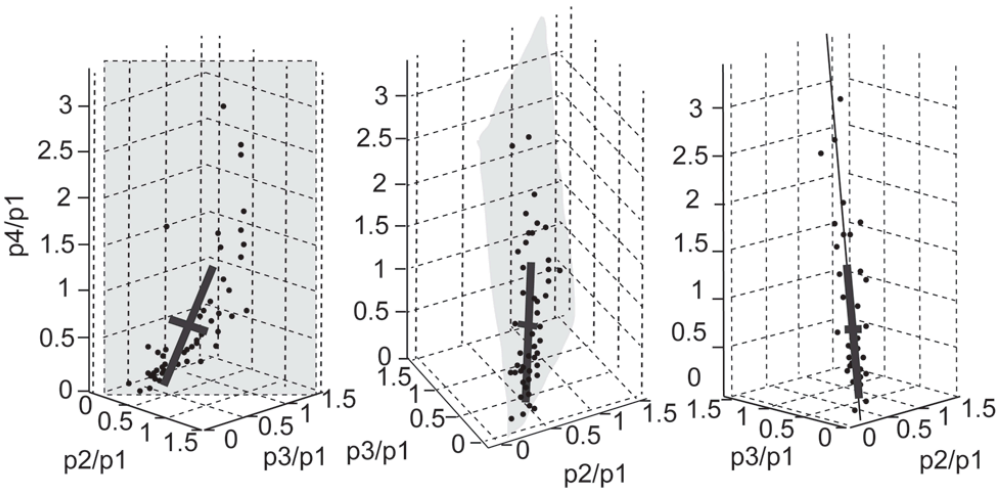

Figure S4. Three dimensional morphospace of digit 4 phalanges. Principal component analysis of the birds dataset. Blue lines depict the three principal components; line length corresponds to the standard deviation (STD) of each component. Crossing point is at average of data in the three axes.

Generating a randomized data set

In a similar fashion to the line criteria discussed above, we obtain a significance measure for the plane criterion of a dataset, by comparison to a null model made of an ensemble of suitably randomize datasets. Each randomized data set preserves the statistics of each trait, but that reflects a situation where the traits are independent of each other. Again, each dataset is comprised of the same number of points N as the original dataset, where x, y, and z values are drawn from the corresponding CDFs. An example of a randomized dataset produced with this procedure for the birds dataset is shown in Figure S5. For each randomized data set, the variance ratio of components 3 and 2 is computed. v_r of the randomized dataset is 0.58, showing that it is less planer than the original dataset.

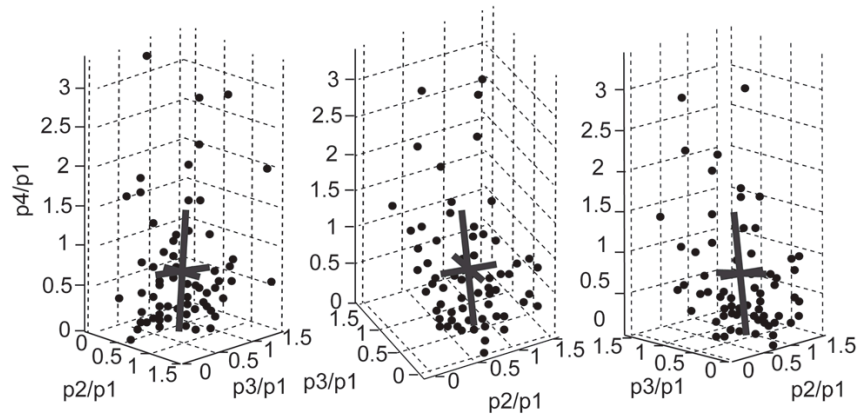

Figure S5. Randomized dataset. Blue lines depict the three principal components of the randomized dataset.

Computing the p-value

To find the p-value for how well the data falls on a plane, we compute v_r of the original dataset, and compare to 10,000 randomized datasets. The z-score is 5.4.

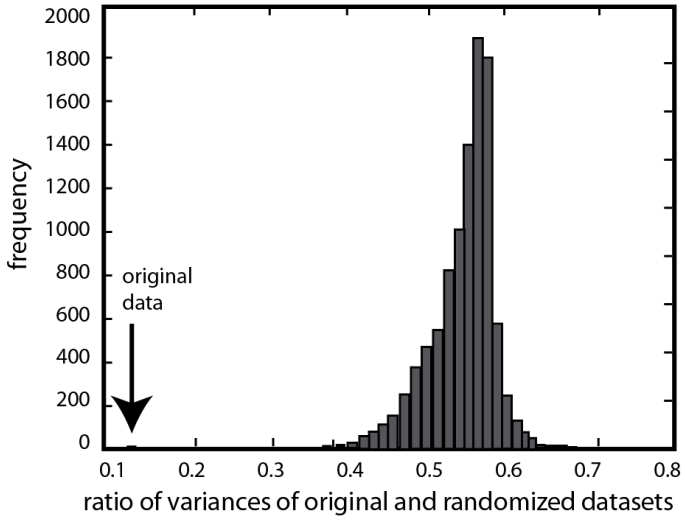

Figure S6. Histogram of v_r for 10,000 randomized data sets. The original dataset has a v_r lower than all randomized dataset, leading to a p-value $< 10^{-4}$.

Extension: calculating whether the Z plane is off the vertical

If the value of the third trait (p4/p1), which is displayed on the z-axis, is not dependent on the other two traits (p2/p1, p3/p1), that represent the x-y axes, we would expect the best-fit plane to be vertical. This would imply that p4/p1 varies independently from p2/p1 and p3/p1. Here we provide a test that examines whether the best-fit plane is off the vertical, and provides a p-value.

First, we define a measure of how vertical is the best-fit plane, which is calculated using principal component analysis. The best-fit plane is found using the first two components. Consider the 3rd principal component, which is perpendicular to the best-fit plane (principal components are always perpendicular to each other). Note that if the 3rd component is parallel with the x-y plane, then the best-fit plane is perpendicular to the x-y plane. Thus, we can use the ratio of the z-value and the x-y values of the 3rd principal component, to determine how vertical is the plane.

In order to test for a p-value, we create randomized datasets as described above. For each dataset we compute the ratio *l*, and compare with the ratio of the original dataset, to get the p-value.

1C. Tests for whether a 2-trait dataset stems from the same distribution as another dataset

Consider the birds (primary) and cetacean (secondary) datasets depicted in Figure S7. Here we present several methods for testing whether the cetacean dataset stems from the same distribution of the birds dataset.

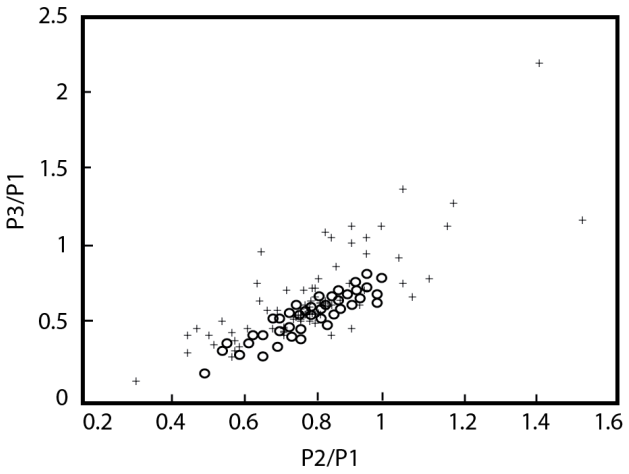

Figure S7. Digit III ratios for the birds dataset (grey dots), and the cetacean dataset (black circles).

A test of whether the secondary dataset is aligned with the primary dataset

We begin by performing principal component analysis of the main dataset (birds in our example, Figure S8A). The percent variance of the second dataset along the first principal component axis of the main dataset is a measure of the alignment of the two datasets (Figure S8B). Next we create randomized datasets based on the statistics of the second dataset (in a similar fashion to the randomizations described above). Each randomized dataset has the same number of measurements as the original dataset, and the same x and y distributions. For each randomized dataset the percent variance along the first principal component of the main dataset is computed (Figure S8C). These results are compared with the values for the original dataset to compute the p-value.

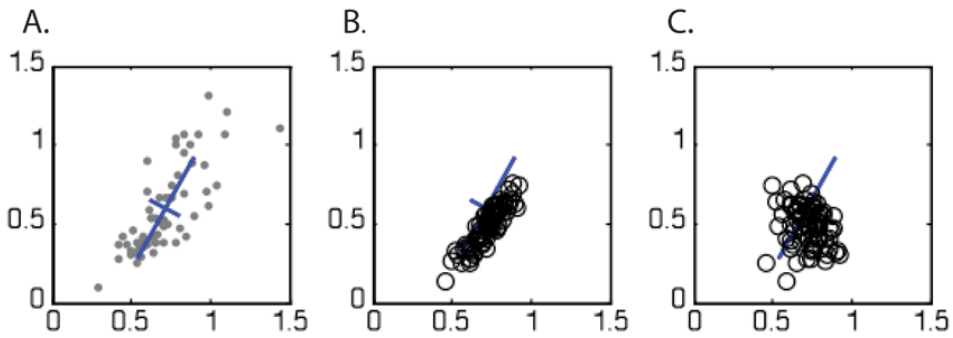

Figure S8. A. Main dataset, and the principal components (blue lines). B. Secondary dataset, with principal components of main dataset. C. Randomized dataset with principal components of main dataset.

A test of whether the secondary dataset is not centered along the primary dataset

The two datasets might be aligned, but parallel, in the sense the intercept is significantly different. Here we present a method of testing whether the secondary dataset is not centered along the primary dataset, in a statistically significant manner.

First the principal components of the primary dataset are computed. For each datapoint j in the secondary dataset, we find the distance d_j from the line defined by the 1st principal component of the main dataset (Figure S9, black lines). The distribution of d_j for the birds and cetaceans example is shown in Figure S9. Note that the distribution is not centered at zero - if the secondary dataset was centered on the main dataset, the mean of the distances would be zero. We now perform a t-test, which tests whether the data in vector d_j has a mean that is not zero. The t-test returns the confidence level, where the standard threshold used is 5%. Thus, if the t-test returns a value higher lower than 5%, than we can reject the hypothesis that the secondary dataset is centered with the main dataset. In this case, the t-test returns 0 – indicating that there is a high probability that the mean of the dataset is not zero, which implies that the two datasets are not centered on the same line.

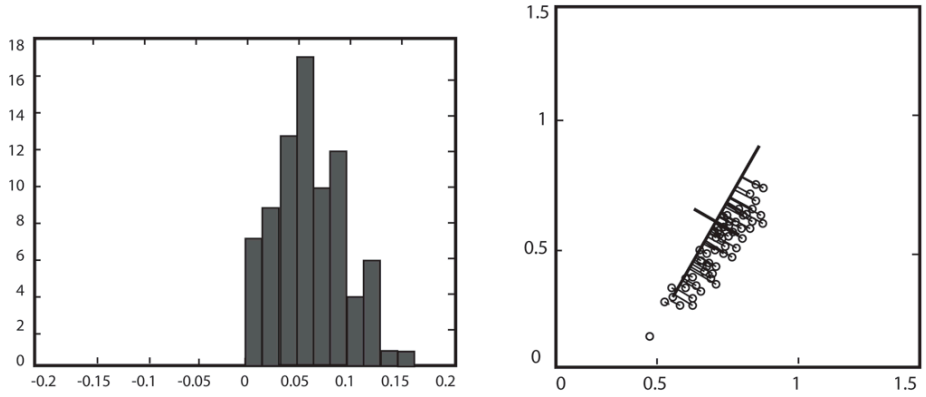

Figure S9. A. Cetaceans dataset, and principal components of the birds dataset. For each datapoint the distance from the 1st principal component is shown by a black line. B. Distribution of distances of datapoints from 1st principal components.

Conducting these Tests on particular datasets:

1D. Results for Bird populations (Chicken and Zebrafinch) for Digit IV, P1-3

Do phalanges vary independently in bird populations?

Figure S10 depicts the variation of the phalanges' proportions of the bird populations. Using the statistical method described above, we find that the phalanges ratios are dependent (p-value < 10^{-4}).

Among chick individuals, using the same test, we find that variation in proportions is not random (p-value < $2*10^{-4}$).

Among zebrafinch individuals, similarly, we find that the variation is not random, with p-value < 10^{-4}.

Are proportion variants within populations similar to proportion variants among species?

Among chick individuals, variation is not different from dataset among all birds: both data sets are aligned (p-value < $2*10^{-4}$), and their means cannot be distinguished (ttest>0.05).

Among zebrafinch individuals, variation is not different from among all birds: both data sets are aligned (p-value < 10^{-4}), and their means cannot be distinguished (ttest>0.05).

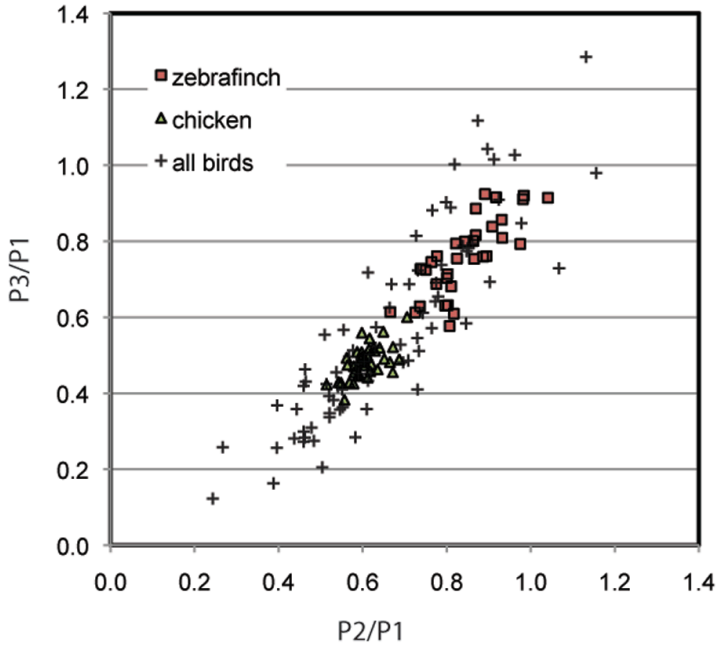

Figure S10. Phalanges proportions for Digit IV, P1-P3 for zebrafinch and chicken populations and means of 76 species of birds.

1E. Results for Major taxonomic group proportion variants

Do phalanges proportions vary independently in vertebrate groups?

No, variation is not random. They all fall on a line from proximo-distal gradient to equal-sized (see p-values in table below).

Is the range of phalanges proportion variants in all major vertebrate taxonomic groups similar?

Among birds, lepidosaur reptiles, lissamphibians, ichthyosaurs, plesiosaurs, and cetaceans, there is no detectable difference in slope. In some groups there is a significant difference in intercepts (see table below with statistical results).

Taxon	Distribution not random p-value	Aligned with the SARC group p-value (similar slope)	Mean distinguishable from SARC group (similar intercept)
Birds	$<10^{-4}$	$<10^{-4}$	Yes
lepidosaur reptiles	$<10^{-4}$	$<10^{-4}$	Yes
lissamphibians	$<10^{-4}$	$<10^{-4}$	No
ichthyosaurs	$<10^{-4}$	$<10^{-4}$	Yes
plesiosaurs	$<10^{-4}$	$<10^{-4}$	No
cetaceans	$<10^{-4}$	$<10^{-4}$	Yes
early SARC	$<10^{-4}$	-	-

1F. Results for Bird species P1-P4

Do phalanges proportions in birds fall along a plane in morphospace?

Yes (p-value$<10^{-4}$).

Statistical significance of digit IV data being on a plane (test 1B)

Fig. 5 in the main text depicts the ratios of phalanges' areas relative to the area of phalanx 1. In three perspectives of this 3 dimensional plot we see that the data is limited to a plane. Using principal component analysis we find the relative variances of the three principal components are 85.2%, 12.4%, and 2.4%. The low variance of the 3rd component mathematically shows that the data fall on a plane. Here we examine the statistical significance of this finding, and evaluate what is the probability that if the

different phalanges were drawn from unrelated distributions, we would get such a result. In summary, using the bootstrapping method, we build a new dataset of the safe size, with 65 samples, where for each sample, the phalanges area ratios are drawn randomly from their distribution. See detailed explanation below.

After normalization by the first phalanx, the data has three variables: p2/p1, p3/p1, and p4/p1. We denote them by A, B and C respectively. There are a total of 65 sample points in the data, each one with a value for A, B and C. in order to compare the three variables in the same scale, we normalize each by its standard deviation (z-score). Using the bootstrapping method, we draw by random a value from A, a value from B and a value from C. This creates a new sample that has phalanges' ratios chosen from three random birds' measurements. This step is repeated 65 times in order to create a data set the same size as the original one. In order to examine if the data in this randomized data set also falls on a plane, principal component analysis is used, and the variance of the third component is analyzed. The above analysis is repeated 10,000 times to get a distribution of the measure of the variance of the third principal component. This distribution has a mean value of 24%, and a standard deviation of 3%. The original data set gives us a variance of 2.4% for the 3rd principal component, which is 7 standard deviations from the mean. For a normal distribution the corresponding p-value is $6.5*10^{-13}$.

In summary, if there was no relationship between phalanges' areas, the probability of finding the data set falling on a plane is extremely low.

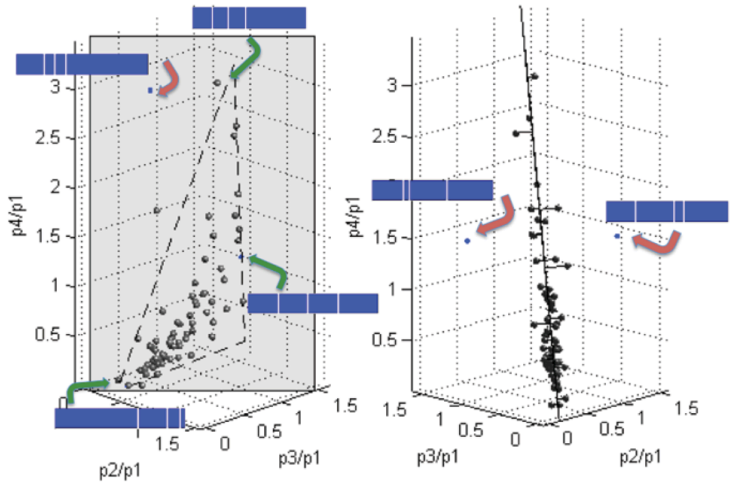

Figure S11. Two rotations of 3D morphospace showing proportions of bird Digit IV phalanges P1-P3 (dots). Dashed triangle shows area generally covered by the range of variation in proportions for this digit. Blue rectangles illustrate proportions; left is proximal. Green arrows point to proportions of some observed species. Red arrows point to proportions that are off the plane or outside the observed range, thus apparently not found in nature.

1G. Statistical significance of digit 4 data being on a plane (test 1B)

Is the Z-plane off the vertical?

Yes, slightly but significantly, indicating P4 variation is also linked to the size proportions of the other phalanges.

1H. Results for Darwin's finches

Arboreal species of Darwin's finches have significantly more elongated P4 phalanges than ground species. The overall proportions of Darwin's finches fall within the plane defined by proportions from all birds.

SOM 2: Developmental methods and analyses

Kathryn Kavanagh, Benjamin Winslow, and Akinori Kan

2A. Time for formation of a phalanx from proximal to distal joint interzone.

The final proportions of the phalanges are established during the period of sequential joint formation in the embryo, occurring over about three days of development in the chick. Final proportions of Emu, Chick, and Barn Owl, three species with very different proportions, are observable at the time of tip formation (Figure S12). Individual phalanges are established between the time when the proximal joint interzone forms and when the distal joint interzone appears. Regulation of the time between sequential joint interzone formation during this period is thus potentially one of the developmental mechanisms that regulates final proportions in the digit.

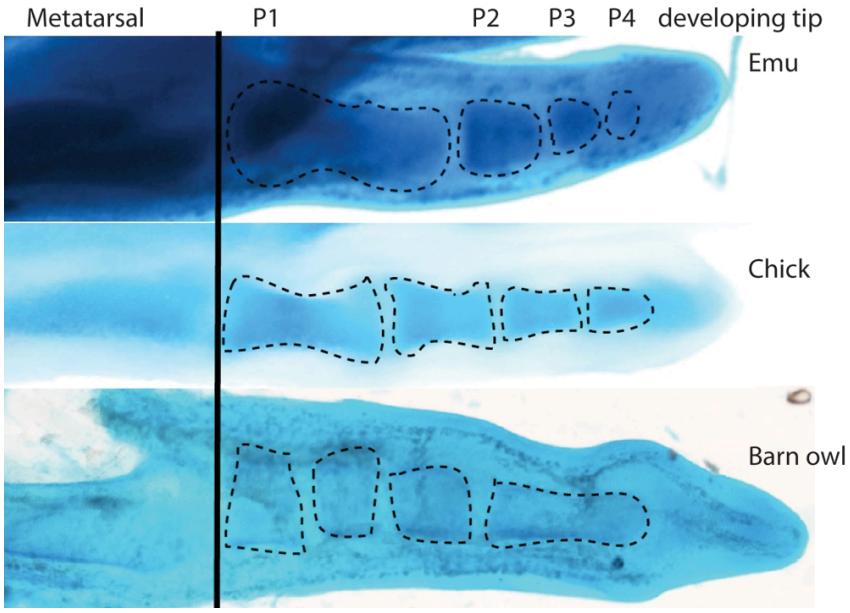

Figure S12: Late phalanx development in emu, chick, and barn owl embryos, just before tip is formed. This demonstrates that the proportions are determined during this morphogenetic phase and not due to post-morphogenetic growth differences.

To calculate number of hours from formation of proximal joint to distal joint in a phalanx, which is the period of patterning and developmental plasticity for that phalanx, we performed the following steps:

Method 1: Time series

1. Over several months, we obtained batches of fertilized chick eggs (>20 batches; Charles River Labs), which had been collected from nests over several hours and cooled to 18°C. Soon after they were received, the entire batch began 38°C incubation to initiate synchronous development.
2. We collected and fixed groups of three embryos at intervals (usually 2-hrs) throughout digit developmental stages.
3. Embryos were KOH cleared and Alcian stained. Distal limbs were removed from the embryos and then photographed from a dorsal (top) view.
4. The 2D area of each developing phalanx (Alcian stained area) was measured using ImageJ. Stage of joint formation in Digit IV recorded as a way of staging digit development so that equivalent stages could be compared.
5. Average condensation area for each phalanx was calculated.
6. All condensation sizes were aligned to find the smallest initial condensation size; the sample size was determined to be sufficient if the smallest 5 condensations do not differ more than ~5%.
7. In order to find the condensation size at which the distal joint of a given phalanx is formed, we determined the size of a given phalanx at the time when the next phalanx has the smallest initial condensation observed (since that is immediately after the joint interzone is formed).
8. The growth rate of a given phalanx was determined by examining phalanx condensation size increase over time in our series, and dividing by the number of hours between collections.
9. The number of hours to form a given phalanx was then calculated by dividing the growth rate by the difference in size between initial condensation and the condensation at the time of distal joint formation.

[(Area at t2) – (area at t1)] / (growth/hr) = # hrs

t=time

Method 2: Chick embryo cut-foot pairs

1. Chicks were incubated to day 7 or 8.
2. A window was opened in the egg and amnion, avoiding blood vessels. One hindlimb autopod was removed with micro-scissors for fixation, and the egg was returned to the incubator with tape over the window.
3. The embryo was allowed to incubate an additional 6-48 hrs before collecting/fixing the other hindlimb autopod.
4. Limbs were Alcian stained and KOH cleared.
5. The number of additional joints was determined by counting the areas of clear tissue (no Alcian stain) indicating the developing joint interzones. The difference in condensation size for a given phalanx between first and second collection was measured.
6. The maximum number of hours before a new joint is observed in a digit was determined as an estimate of the number of hours to form a given phalanx.

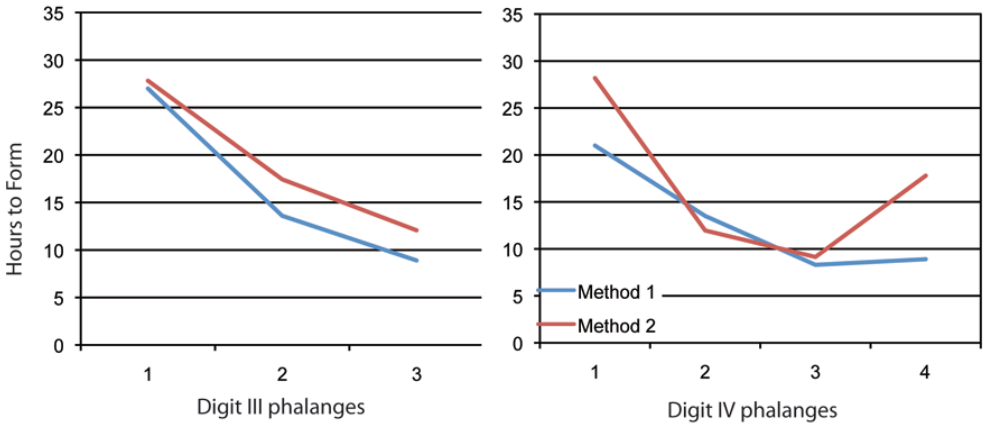

Figure S13: Average time of formation (number of hours between proximal and distal joint interzone formation) for phalanges of Digit III (left) and Digit IV (right).

2B. Proliferation study

We injected 400µl of 1mM EdU solutions into amniotic fluid, and harvested embryos 6 hours after the injection. We made a paraffin section and used Click-iT EdU Alexa Fluor 555 Imaging kit (Invitrogen) for imaging as previously reported (Dev Dyn. 238:944–949, 2009). Proliferation rates were calculated by counting numbers of labeled cells in 200um quadrants.

2C. Barrier experiments

Pre-cut tantalum foil barriers were implanted into digit IV of the right hindlimb using forceps during day 5 (metatarsal barriers) or days 6-7 (phalanges barriers) of development. To perform the microsurgeries eggs were windowed, the amniotic sac was opened with forceps, and the hindlimb was placed on a dark paper stage to provide contrast. Barriers were inserted through the distal end of the digit condensation, after which the limb was returned to the amniotic sac. Penicillin/streptomycin was then added, the egg was sealed with tape, and returned to the incubator. Eggs were incubated until day 10 or 11, when embryos were collected and fixed in formalin over night. Feet were removed and stained for cartilage with Alcian blue, then cleared in KOH.

Wound controls were conducted exactly as above, except that foil barriers were inserted and then removed after ~ 1 minute.

Cleared and stained feet were photographed, and the fourth digits from the experimental and contralateral feet were aligned using Adobe Photoshop. For metatarsal barriers, pairs of digits were visually inspected to determine if the metatarsal was noticeably shortened, and if clear changes occurred to the phalanges.

To determine if phalanges were affected in wound control barriers, first the amount of variation between the same phalanx on the left and right foot in normal embryos was assessed. The area of each phalanx was measured using ImageJ software, and the percent difference of each phalanx was determined for 19 normal chick embryos at day 10-11. From these measurements the average percent difference for all pairs of phalanges was calculated (9.4%), as was the standard deviation (7.7%). The percent

difference between experimental and contralateral control phalanges sizes were then compared to left-right variation observed in normal embryos. Specimens were scored based on if phalanges size differences exceeded the average amount by more than 1, or more than 2 standard deviations. 33/45 (73%) of the experimental digits contained phalanges where the percent difference from the contralateral side exceeded the average plus 1 standard deviation, and 29/45 (64%) exceeded the average percent difference by more than 2 standard deviations. In wound controls, only 4/13 (31%) digits contained phalanges that exceeded the average percent difference plus 1 or 2 standard deviations. Images of wound controls and phalanges experimental barriers were also aligned in Photoshop and assessed visually.